JACS
JOURNAL OF THE AMERICAN CHEMICAL SOCIETY

Article

pubs.acs.org/JACS

# Enantiodivergent Fluorination of Allylic Alcohols: Data Set Design Reveals Structural Interplay between Achiral Directing Group and Chiral Anion

Andrew J. Neel,[†,∥] Anat Milo,[‡,§,∥] Matthew S. Sigman,[*,‡] and F. Dean Toste[*,†]

[†]Chemical Sciences Division, Lawrence Berkeley National Laboratory, and Department of Chemistry, University of California, Berkeley, California 94720, United States

[‡]Department of Chemistry, University of Utah, 315 South 1400 East, Salt Lake City, Utah 84112, United States

[§]Department of Chemistry, Ben-Gurion University of the Negev, Beer Sheva, 84105, Israel

Supporting Information

**ABSTRACT:** Enantioselectivity values represent relative rate measurements that are sensitive to the structural features of the substrates and catalysts interacting to produce them. Therefore, well-designed enantioselectivity data sets are information rich and can provide key insights regarding specific molecular interactions. However, if the mechanism for enantioselection varies throughout a data set, these values cannot be easily compared. This premise, which is the crux of free energy relationships, exposes a challenging issue of identifying mechanistic breaks within multivariate correlations. Herein, we describe an approach to addressing this problem in the context of a chiral phosphoric acid catalyzed fluorination of allylic alcohols using aryl boronic acids as transient directing groups. By designing a data set in which both the phosphoric and boronic acid structures were systematically varied, key enantioselectivity outliers were identified and analyzed. A mechanistic study was executed to reveal the structural origins of these outliers, which was consistent with the presence of several mechanistic regimes within the data set. While 2- and 4-substituted aryl boronic acids favored the (*R*)-enantiomer with most of the studied catalysts, *meta*-alkoxy substituted aryl boronic acids resulted in the (*S*)-enantiomer when used in combination with certain (*R*)-phosphoric acids. We propose that this selectivity reversal is the result of a lone pair-$\pi$ interaction between the substrate ligated boronic acid and the phosphate. On the basis of this proposal, a catalyst system was identified, capable of producing either enantiomer in high enantioselectivity (77% (***R***)-**2** to 92% (***S***)-**2**) using the same chiral catalyst by subtly changing the structure of the achiral boronic acid.

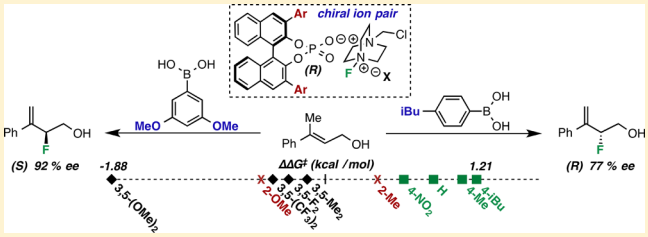


## INTRODUCTION

The *de novo* design of chemo-, regio-, and stereoselective catalysts remains an ongoing challenge in the field of organic synthesis. In the case of enantioselective catalysis, a key issue is the influence that catalyst and substrate structural features have on product enantiomeric excess (ee) due to interactions at the transition state (TS). This issue is exacerbated in situations where seemingly minor perturbations to the catalyst or substrate structure have a profound, and often nonintuitive, influence on enantioselectivity. Conversely, this very feature establishes the measurement of enantioselectivity as a powerful mechanistic probe. Assuming that the conditions of the Curtin−Hammett principle are satisfied,[1] a product's observed enantioenrichment can be related to the free energy difference between the competing diastereomeric TSs leading to either enantiomer ($\Delta\Delta G^{\ddagger} = -RT \ln[(S)/(R)]$ in kcal/mol). Thus, enantioselectivity represents a relative rate measurement that is sensitive to the structural features of each reacting component. Considered from this perspective, every selectivity value obtained in the course of data collection bears specific structural information regarding the mechanism of asymmetric catalysis.

We recently reported a strategy to exploiting this wealth of mechanistic information.[2] Briefly, this approach involves (1) preparing a catalyst and substrate library of systematically perturbed structures, (2) identifying molecular descriptors that could serve to quantify these structural changes, (3) correlating these molecular descriptors with experimental selectivity outcomes of each catalyst and substrate combination in the data set, (4) developing mechanistic hypotheses on the basis of the descriptors required for modeling, and (5) preparing tailored catalysts or substrates to probe these hypotheses. Using this approach, the key noncovalent interactions underlying asymmetric induction[3] were hypothesized, and consequently a series of catalysts that leveraged these putative interactions to improve selectivity over the entire data set were prepared and validated.[2]

**Received:** January 11, 2016
**Published:** March 11, 2016

ACS Publications © 2016 American Chemical Society



DOI: 10.1021/jacs.6b00356
J. Am. Chem. Soc. 2016, 138, 3863−3875

Although this strategy is general for the study of selective reactions, it is predicated on the assumption that any variation in selectivity stems from an analogous mechanism of asymmetric induction for each data set member. If this assumption is not valid for certain examples in the data set, they cannot be directly compared. Classically, such changes in mechanism have been revealed through changes in the slope of univariate correlations (e.g., Hammett plots).[4−23] However, in cases where multivariate correlations are applied, these changes become more challenging to identify, because the parameters employed could serve to account for this variance.[7] We became interested in the question of how changes in mechanism could be identified in such scenarios, as this would allow for further generalization of our strategy that uses focused data sets to elucidate the structural origins of enantioselectivity. Herein, we demonstrate how data set design and organization enable the rapid identification of mechanistic breaks that can be subsequently confirmed experimentally. This approach allows for valid comparisons to be made within a data set, resulting in the identification of reasonable structural origins of enantioselectivity under different mechanistic regimes. As a demonstration of the insight gained, we have rationally designed a catalyst system capable of producing either enantiomer of a chiral fluorinated product in high enantioselectivity using the same enantiomer of chiral catalyst with a different achiral additive.[24−26]

Recently, our group described the concept of chiral anion phase transfer (CAPT) catalysis (Figure 1A).[27−49] This strategy relies on employing an insoluble cationic electrophile in a nonpolar organic solvent, thus minimizing the unselective background reaction with a soluble substrate. The electrophile is solubilized through the action of a chiral, lipophilic, anionic phosphate salt,[50−54] ensuring that it is in a chiral environment when it encounters the substrate in solution. This strategy has proven successful for several electrophiles, including diazonium salts,[43,44,47] oxoammonium salts,[36,38] and halogenating reagents (Selectfluor along with its bromo and iodo analogues). With respect to this latter reagent class, although a number of examples have been reported by our group[30−35,37,42] and others,[39−41,45,46,48,49] enantioselectivity has typically depended on a preinstalled directing group to facilitate the interaction between the substrate and phosphate catalyst in the enantiodetermining step.

To address this limitation, it was recently demonstrated[55] that simple allylic alcohols could be fluorinated[56−63] with ee values of up to 94% using aryl boronic acids (BAs) as traceless, *in situ* directing groups (Figure 1B).[64] The essential role of the aryl BA for high enantioselectivity was underlined by the formation of racemic product in its absence. However, it was observed that enantioselectivity was highly dependent on the structure of the aryl BA employed. For example, using **(*S*)-TRIP** as the catalyst, simply changing from 3,5-dimethylphenylboroinc acid to *p*-tolylboronic acid resulted in an 81% change in ee (which, in this case, represents 1.0 kcal/mol, Figure 1C). The notion that selectivity could be influenced to such an extent by an achiral additive is intriguing in terms of the structural underpinnings of this effect. We approached this problem within the framework of our hypothesis that enantioselectivity values can serve as sensitive mechanistic probes that report on specific interactions between reacting partners. Specifically, we anticipated that by designing a data set in which the structural features of the aryl BA and phosphate catalyst were systematically perturbed, we could ascertain the manner in which they interact at the TS to control enantioselectivity in the fluorination of allylic alcohols.

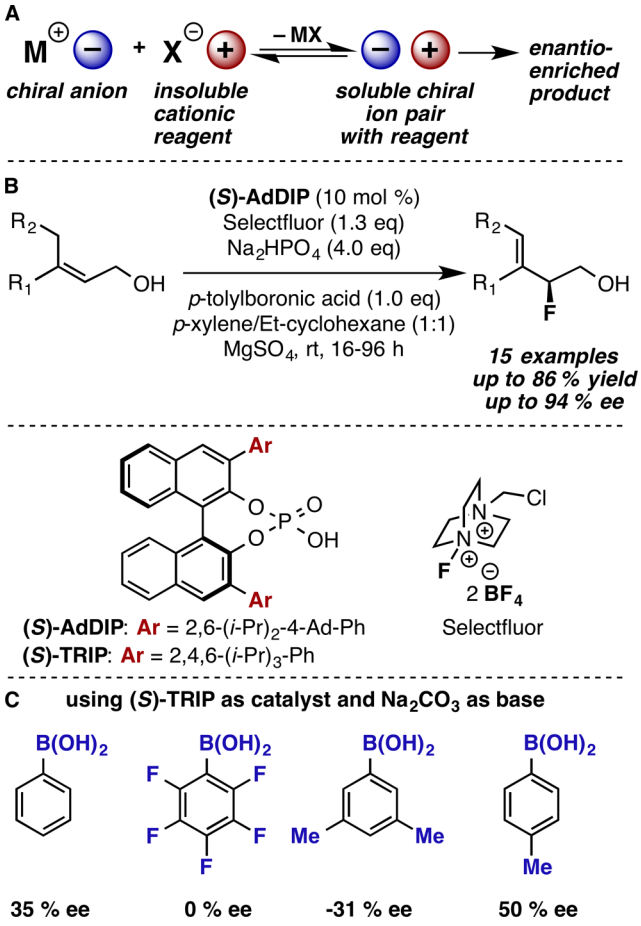


**Figure 1.** (A) Conceptual description of chiral anion phase transfer catalysis. (B) Previously described enantioselective fluorination of allylic alcohols combining a chiral phosphoric acid phase transfer catalyst and a *p*-tolylboronic acid directing group. (C) Enantioselectivity values obtained with different aryl BAs with (*S*)-TRIP.[55]

## RESULTS AND DISCUSSION

**Control Experiments.** Figure 2A depicts our proposed mechanism for this transformation. Following anion metathesis between phosphate **A** and Selectfluor, chiral, soluble ion pair **B** encounters the condensation product (**E**) between allylic alcohol **C** and BA **D**. A concerted or stepwise fluorination-deprotonation sequence in the chiral environment of the phosphate (**G**) affords enantioenriched allylic fluoride **H** and phosphoric acid (PA) **I**, which can be regenerated to the anion by an inorganic base. Prior to initiating our study of the relationship between PA/BA structures and enantioselectivity, we sought experimental evidence that BA monoester **E** was in fact the species undergoing enantioselective fluorination under catalytic conditions. Figure 2B summarizes the relevant results using **(*S*)-TRIP** and *p*-tolylboronic acid as representative reaction components. In the absence of **(*S*)-TRIP**, the yield was greatly diminished (entry 2), supporting its role as a phase-transfer catalyst. Omission of *p*-tolylboronic acid from the reaction mixture somewhat restored the yield, but with a complete loss of enantioselectivity (entry 3). However, a series of NMR titration experiments demonstrated that under relevant conditions, essentially all of alcohol **1** is associated


DOI: 10.1021/jacs.6b00356
J. Am. Chem. Soc. 2016, 138, 3863−3875

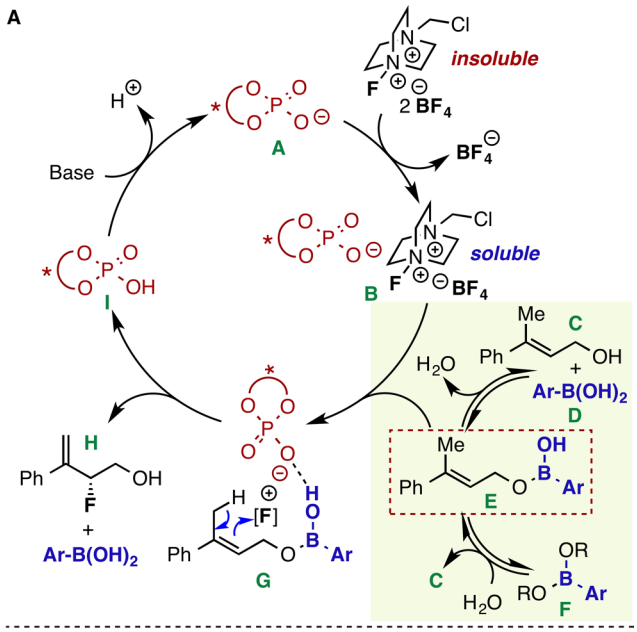


| entry | Omitted Reagent | yield (%) | ee(%) |
|---|---|---|---|
| 1 | none | 52 | 66 |
| 2 | (*S*)-TRIP | 5 | -- |
| 3 | *p*-tolylboronic acid | 39 | 5 |
| 4 | MS 4A | 62 | 66 |

**Figure 2.** (A) Proposed catalytic cycle for chiral PA catalyzed enantioselective fluorination of allylic alcohols. (B) Control experiments supporting *p*-tolylboronic acid's role as a directing group. All reactions were conducted on 0.1 mmol scale with respect to allylic alcohol **1**.

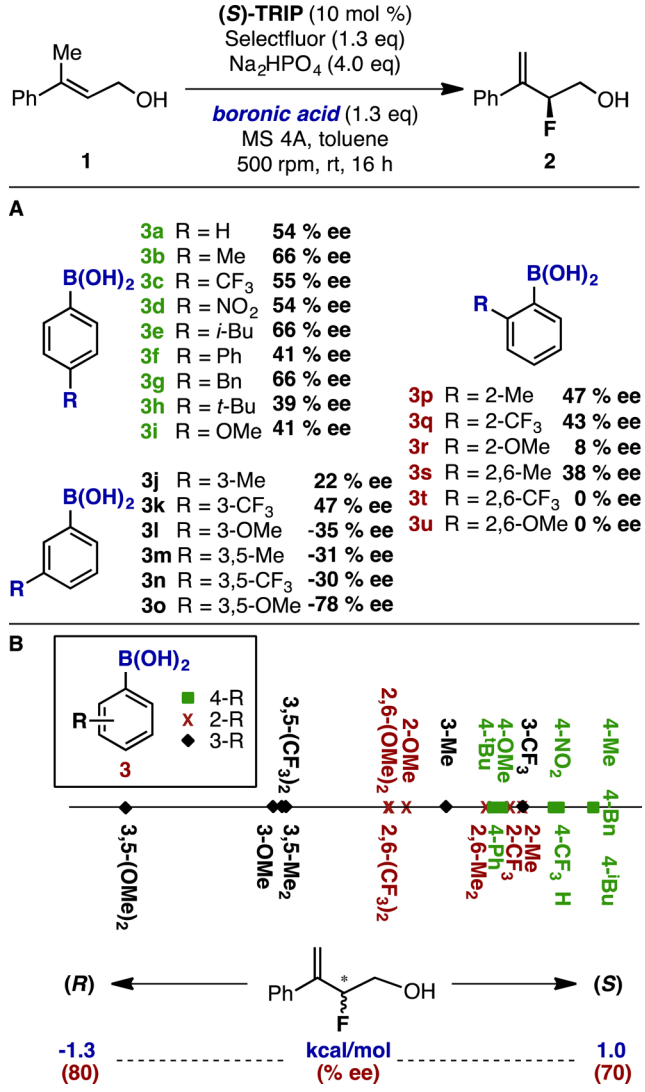


**Figure 3.** (A) Effect of boronic acid structure on enantioselectivity. All reactions were conducted on 0.05 mmol scale with respect to allylic alcohol **1**. (B) Visualization of enantioselectivity range of **2** attainable by variation of boronic acid structure.

with BA, either as the *mono*- (**E**) or *bis*-ester (**F**, see Supporting Information for details), suggesting that this unselective pathway is likely inoperative under catalytic conditions. Finally, omission of molecular sieves resulted in an increased yield, while enantioselectivity remained unaffected.[65] The diminished yield in the presence of molecular sieves likely arises from the increased formation of BA *bis*-ester **F** under these dehydrating conditions, which serves as an unreactive reservoir of alcohol **1**. Collectively, these data sufficiently demonstrate that monoester **E** is likely the relevant species interacting with the chiral phosphate in the enantiodetermining step of this reaction. The remainder of our study was devoted to uncovering the nature of this interaction within the relatively opaque region of the catalytic cycle from **E** to **G** to yield **H** (Figure 2A).

**Data set Design.** Prior to designing a data set in which both BA and phosphate structures were systematically modified, we sought to establish the enantioselectivity range accessible by changing only the achiral aryl BA. It was reasoned that this approach would allow us to rapidly identify which BA structural features most affected enantioselectivity, enabling the effective design of a data set of catalysts and BAs. To this end, 21 commercially available aryl BAs were selected with substituents that systematically spread the reaction space with respect to both their steric and electronic profiles at the 2-, 3-, 4-, 2,6-, and 3,5- positions of the aryl ring (Figure 3A-B). (*S*)-**TRIP** was selected as the catalyst for these studies, given its ubiquity in the field of chiral PA/phosphate catalysis.[66,67] Using conditions slightly modified from those previously reported,[65] the enantiomeric excess of **2** was measured using each of these BAs with (*S*)-**TRIP**, resulting in values ranging from 66% ee of the expected (*S*)-**2**, to 78% ee of the (*R*) enantiomer. Remarkably, this represents a 2.2 kcal/mol range based solely on the structure of the achiral BA (Figure 3B).

A notable structural effect is apparent from these data as well: 4-substituted phenyl BA derivatives lead to the (*S*) enantiomer with the largest ee values, followed by their 2- and 3-substituted counterparts, with 3,5-substituted derivatives resulting in the highest enantioselectivities favoring the (*R*) enantiomer.

Having established this range, we turned to design a complete data set in which both BA and phosphate structures were perturbed (Figure 4A). To this end, eight BAs were selected that evenly covered the range of enantioselectivities representative of the different substitution patterns that were


DOI: 10.1021/jacs.6b00356
J. Am. Chem. Soc. 2016, 138, 3863−3875

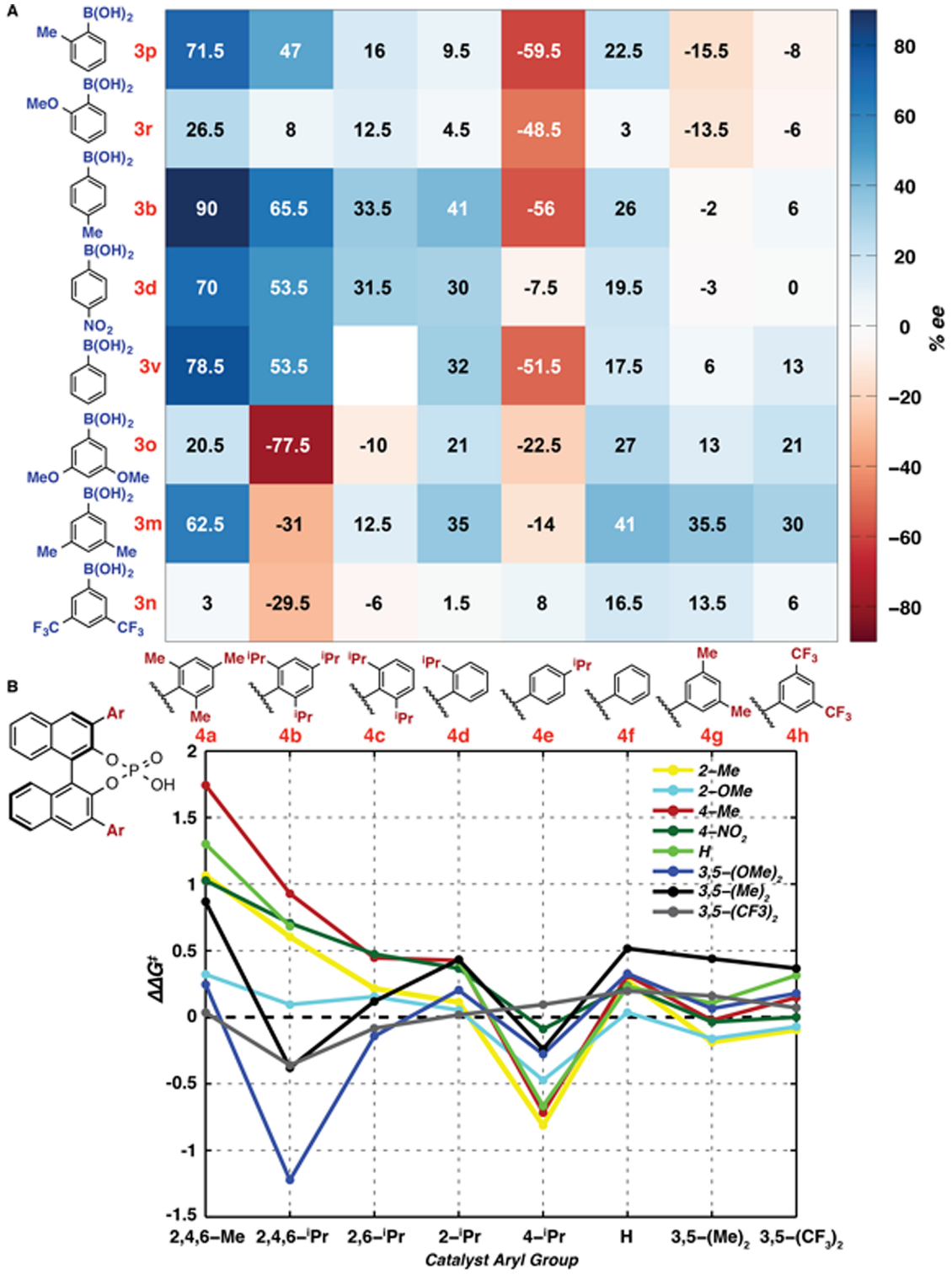


**Figure 4.** (A) Enantioselectivity data obtained by variation of PA and BA substitution pattern. All reactions were conducted using 0.050 mmol **1**, 0.065 mmol **3**, 0.065 mmol Selectfluor, 0.200 mmol $Na_2HPO_4$, 0.005 mmol **4**, and 40 mg MS 4Å in toluene (0.1 M). (B) Graphical representation of BA structure−selectivity trends as a function of catalyst structure.

believed to influence selectivity (i.e., 2-, 4- and 3,5-substituted). Simultaneously, eight phosphate catalysts were prepared with variable substitution at the 3 and 3′ positions of the binaphthyl backbone. Mesityl-substituted catalyst **4a** was selected as a less-encumbered version of **TRIP** (**4b**) to assess the potential role of sterics within the 2,4,6-substitution pattern, while 2,6-(*i*-Pr)$_2$-Ph (**4c**), 2-*i*-Pr-Ph (**4d**), and 4-*i*-Pr-Ph (**4e**) substituted catalysts were intended to serve as deconstructed derivatives of **TRIP** to assess any potential isolated effects of these positions. Finally, as the 3,5-disubstituted phenyl BAs **3m**−**3o** had been observed to afford inverted selectivity using **TRIP** as the catalyst (Figure 3), 3,5-disubstituted catalysts **4g** and **4h** were prepared to evaluate the possibility of shape complementarity between the BA and catalyst substituents.



DOI: 10.1021/jacs.6b00356
J. Am. Chem. Soc. 2016, 138, 3863−3875

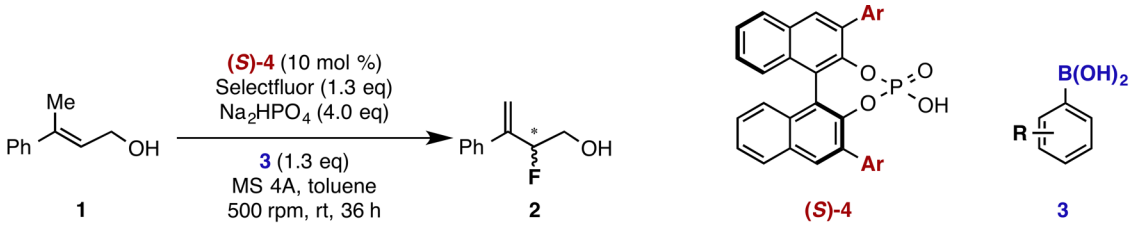


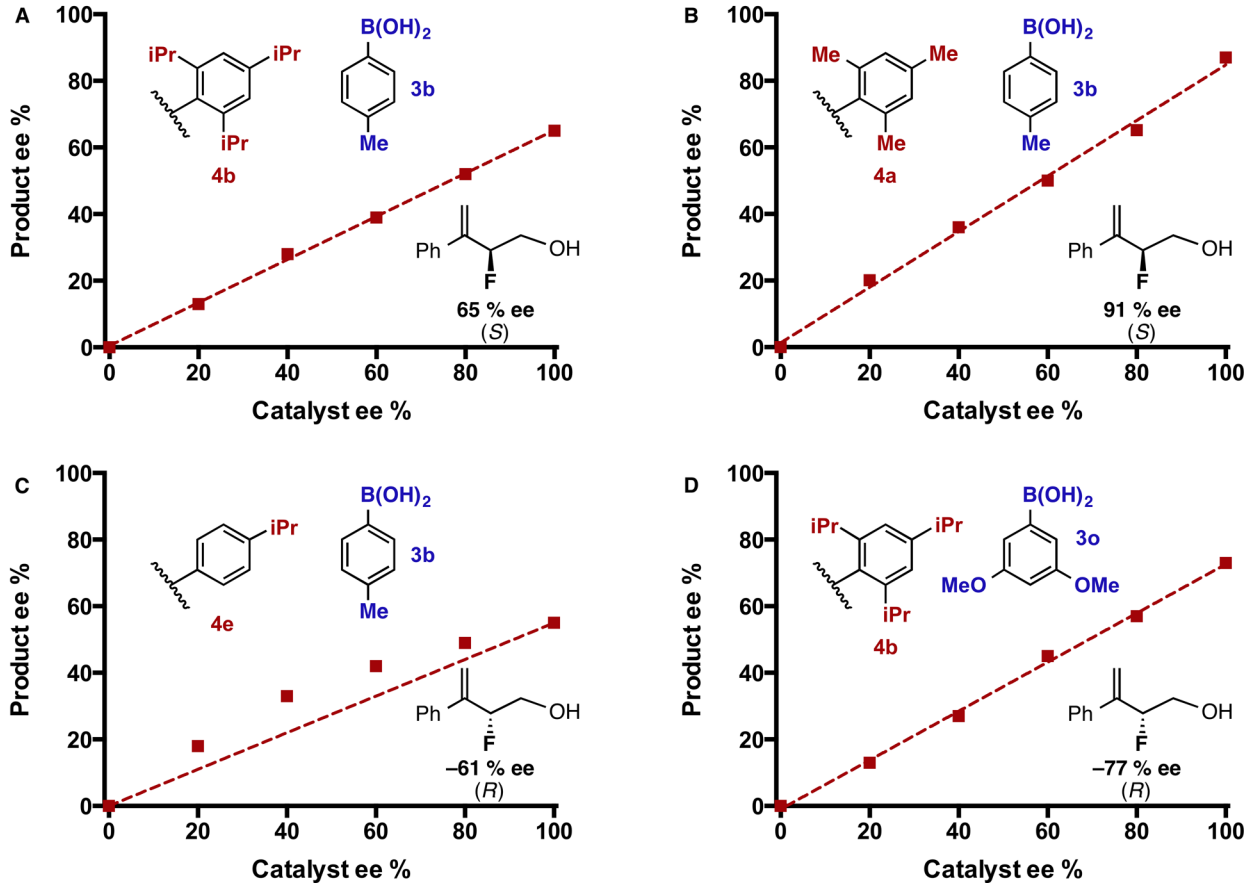


**Figure 5.** Relationship between product and catalyst enantioselectivities for various BA-catalyst combinations: (A) **3b** and **4b**, (B) **3b** and **4a**, (C) **3b** and **4e**, (D) **3o** and **4b**. All reactions were conducted on 0.05 mmol scale with respect to allylic alcohol **1**.

**Data Collection.** With the appropriate libraries of phosphate catalysts and BAs in hand, the enantioselective outcome of each combination was measured with the goal of producing correlations between the experimental values and molecular parameters describing these structural variations.[68−77] Figure 4A depicts the enantioselective outcome of each BA-phosphate combination. It was anticipated that the general trends observed using **TRIP** (Figure 3) would hold across the series of catalysts (e.g., 4-substituted BAs would display the highest propensity for one enantiomer, while 3,5-disubstituted BAs would favor the other). We were therefore surprised to observe that these trends were highly variable from one catalyst to the next, even as a result of seemingly minor structural changes. For example, the use of mesityl-substituted catalyst (*R*)-**4a** resulted in the formation of (*R*)-**2** as the major enantiomer across the entire BA series, in contrast to the use of structurally directly analogous (*R*)-**TRIP** (**4b**), which primarily formed (*S*)-**2** when used in combination with 3,5-disubstituted phenyl BA derivatives. Additionally, the use of catalyst (*R*)-**4e**, in which the *ortho* isopropyl groups of **4b** have been removed, afforded the enantiomeric product (*S*)-**2** across the entire data set. Figure 4B provides a method to visualize these data simultaneously, where each line represents a BA and each *x*-axis tick mark represents a catalyst aryl group. This visualization scheme displays the same information contained in Figure 4A, but in a manner that facilitates the identification of outliers and stark trend breaks. For example, upon moving from left to right, sharp breaks in the observed trends can be detected by distinct, significant changes to enantioselectivity and a reordering of the trend lines.

We have interpreted these sharp breaks in the trends as being indicative of a change in the mechanism of asymmetric induction for certain phosphate-BA combinations. For this reason, although our initial goal was the elucidation of the relevant selectivity-determining interactions across the entire data set through a multivariate correlation, the required models would not necessarily account for these mechanistic breaks. However, we reasoned that a mechanistic understanding of the outliers would contextualize the remainder of the data, allowing meaningful conclusions to be drawn regarding the structural


DOI: 10.1021/jacs.6b00356
J. Am. Chem. Soc. 2016, 138, 3863−3875

origins of selectivity. Because this data set had been designed to cover a broad range of structure enantioselectivity relationships, Figure 4 could serve as a guide for experimentally interrogating regions of the data set that seemed distinctive. Specifically, we were intrigued by the phenomenon that catalysts with the same backbone chirality could deliver either enantiomer of **2** in reasonably high ee. On the basis of the data in Figure 4, this divergence in enantioselectivity appears to manifest itself in two distinct respects: (1) by changing the catalyst substituent (compare (*R*)-**4e**, containing a 4-*i*-Pr-Ph substituent, and (*R*)-**4b**, containing a 2,4,6-(*i*-Pr)$_3$-Ph substituent) and (2) by holding the catalyst constant while changing the achiral BA additive (compare **3b**, 4-Me-Ph BA, with **3o**, 3,5-(OMe)$_2$-Ph BA using (*R*)-**4b** as the catalyst). The ability of the described approach to provide a systematic guide for focused outlier identification steered our further studies toward selecting particular experiments that would reveal the mechanistic possibilities responsible for these observations.

**Nonlinear Effect Studies.** The aforementioned inversions of enantioselectivity are clearly indicative of a major change to the structure of the enantiodetermining TS(s). Given the doubly cationic nature of Selectfluor, we hypothesized that this change may be related to the number of phosphate molecules associated with Selectfluor (i.e., 1 or 2) during C−F bond formation (**B** and **G**, Figure 2A), as this speciation could conceivably be sensitive to the structure of the phosphate, BA or both. To test this possibility, we conducted a series of nonlinear effect (NLE) experiments[78−101] using phosphate/BA combinations from different regions of the original data set hypothesized to function by unique mechanisms (*vide supra*). As depicted in Figure 5A,B, using *p*-tolyl BA **3b**, a linear relationship was observed between catalyst and product ee when using both (*S*)-**4a** and (*S*)-**4b** as catalysts, implicating only a single phosphate in the enantiodetermining TS in each of these scenarios. This result suggests that these two catalyst are directly comparable and that the improvement from 65% ee with **4b** to 91% ee with the structurally analogous **4a** is likely geometric in origin. However, a significant positive NLE was observed using (*S*)-**4e** as the catalyst with **3b** (Figure 5C), which is consistent with the involvement of multiple phosphate species in the enantiodetermining TS.[102] The reduced steric profile proximal to the phosphate moiety in **4e** lends credence to the proposal that this catalyst is more likely to form a dimeric salt compared with the bulkier **4b**.[103] Thus, we propose that the selectivity reversal observed using catalyst **4e** is a result of a fundamentally different mechanism of asymmetric induction when using this catalyst relative to the others in the data set.[104] Intriguingly, a linear relationship between product and catalyst ee was observed using 3,5-(OMe)$_2$-substituted BA **3o** with catalyst **4b** (Figure 5D), a combination that also afforded product **2** with inverted enantioselectivity (−77% ee). This result suggests that a single phosphate molecule is involved in the enantiodetermining TS in this case and therefore, that the origin of selectivity inversion for this particular phosphate/BA combination is different than that of catalyst **4e** (*vide infra*).

**Examination of 4-*i*Pr substituted catalyst 4e.** As 4-*i*-Pr-Ph substituted catalyst **4e** likely operates via an alternative mechanism, the enantioselectivity data collected using it cannot be directly compared with those from the other catalysts in the data set. However, we were interested in the source of the significant variation (8 to −60% ee) in the data obtained using this catalyst resulting from changes in BA structure. To obtain a more complete representation, several additional BAs were evaluated in combination with this catalyst. Figure 6A shows two Hammett plots correlating enantioselectivity to $\sigma_{para}$ that include these results along with those from the original data set. For a given substitution pattern (i.e., 3,5- or 4-), there is an

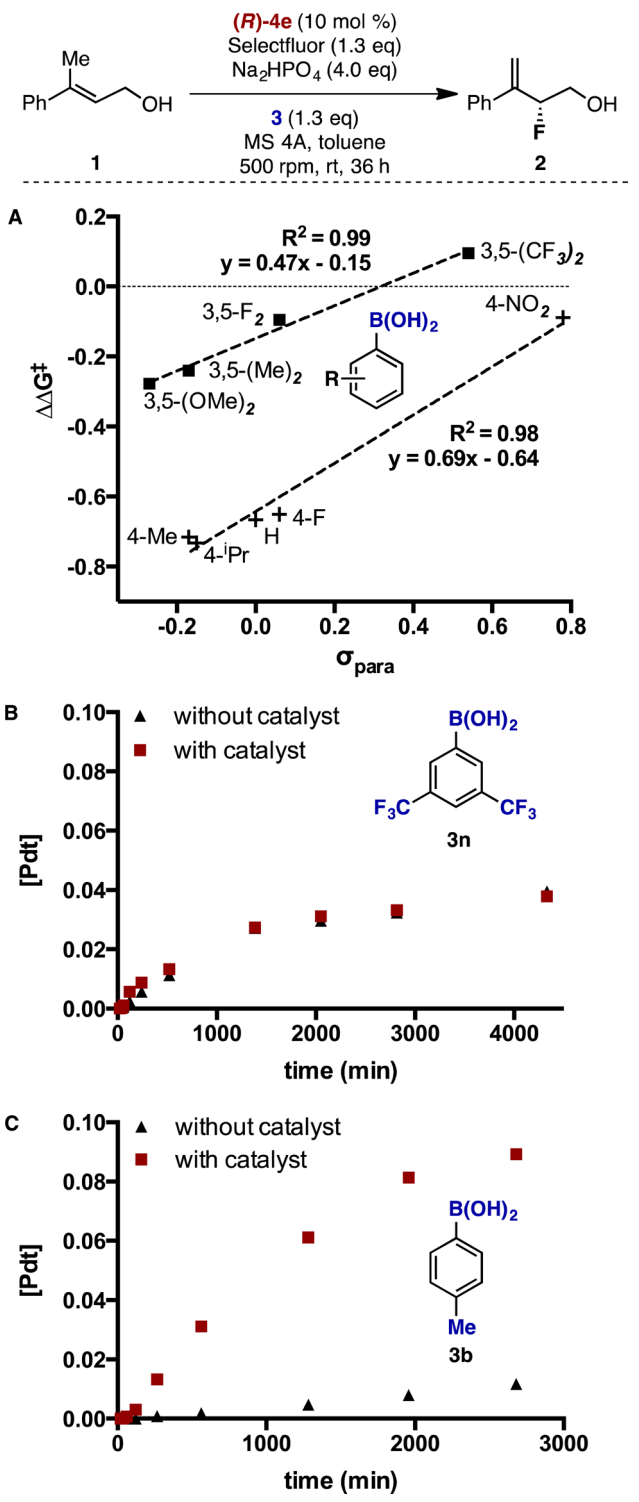


**Figure 6.** (A) Correlation between enantioselectivity of **2** ($\Delta\Delta G^{\ddagger}$) and $\sigma_{para}$ using catalyst **4e** with various boronic acids. All reactions were conducted on 0.05 mmol scale with respect to allylic alcohol **1**. (B) Reaction time course data for formation of **2** using **3n** and **4e** and (C) **3b** and **4e**. All reactions were conducted on 0.1 mmol scale with respect to allylic alcohol **1**.



DOI: 10.1021/jacs.6b00356
J. Am. Chem. Soc. 2016, 138, 3863−3875

excellent correlation between enantioselectivity (represented as $\Delta\Delta G^{\ddagger}$) and Hammett $\sigma_{para}$ values, with electron-rich BAs generally affording higher enantioselectivities than electron-poor examples. The 3,5-substituted BAs cannot be correlated on the same plot as the 4-substituted BAs, yet independently, both plots reveal robust linear free energy relationships with electronic features of the BA substituent.[105]

Martínez-Aguirre and Yatsimirsky recently reported that, in contrast to various other anions, $H_2PO_4^-$ tends to form Lewis acid−Lewis base type tetrahedral adducts with aryl BAs.[106] Furthermore, Tokunaga and co-workers have demonstrated the increased electrophilicity of boron in electron poor aryl BAs by studying the thermodynamics of boroxine hydrolysis as a function of aryl substitution.[107] On the basis of this precedent, we propose that the sterically accessible phosphate moiety in **4e** is inhibited by the formation of a catalytically inactive covalent adduct with electron poor BAs under the reaction conditions. Therefore, the low enantioselectivities observed using electron poor BAs reflect an inability of the phosphate to serve as a phase transfer catalyst and thus to outcompete the unselective background reaction. This hypothesis was probed further by monitoring product formation in the presence and absence of catalyst. As shown in Figure 6B, using 3,5-$(CF_3)_2$-substituted BA **3n**, fluorination occurred at nearly identical rates in the presence and absence of catalyst **4e**. However, using the more electron rich 4-Me substituted **3b**, a rate acceleration over the uncatalyzed background reaction was observed in the presence of catalyst (Figure 6C). Thus, we propose that although the inverted sense of enantioselectivity using **4e** presumably results from the association of two chiral phosphates with Selectfluor, the variation in enantioselectivity observed for this catalyst over a set of BAs is predominantly electronic in origin, with electron poor BAs acting as catalyst poisons.

**Isotopic Substitution Experiments.** Having identified the likely cause for the inverted enantioselectivity displayed by **4e**, we sought a sufficient explanation for the anomalous enantioselectivity observed using **4b** and 3,5-$(OMe)_2$ substituted BA **3o** (−78% ee, Figure 4). The absence of an NLE (Figure 5D), indicated that a single phosphate was presumably involved in this TS. This suggested that the inversion of selectivity relative to 4-substituted BAs was likely due to specific phosphate-BA interactions leading to a change in TS geometry. To gain better insight into this region of the catalytic cycle, substrate **1**-$d_3$ was prepared and subjected to the standard reaction conditions with three different phosphate/BA combinations. As demonstrated in Figure 7, the use of 4-Me substituted BA **3b** with both **4a** and **4b** afforded **2**-$d_2$ with enantioselectivity nearly identical to that observed with its protonated analogue. However, the combination of **3o** and **4b** provided **2**-$d_2$ in −90% ee, a 13% ee (0.5 kcal/mol) increase relative to **2**. These results suggest that the cleavage of the C−H bond is involved in the enantiodetermining TS in the latter case, but not in the former. Figure 7B depicts a plausible mechanistic explanation for this situation, in which a continuum exists between two limiting scenarios: (1) irreversible, enantiodetermining fluorination followed by rapid deprotonation (pathway a) or (2) concerted enantiodetermining fluorination-deprotonation (pathway b). The enantioselectivity differences between the deuterated and protonated substrate along this mechanistic continuum depend on the substituents of the aryl BA, and are suggestive of a specific interaction between the BA and catalyst in the latter of the two limiting scenarios. The absence of an effect in the case of **3o** with **4a**

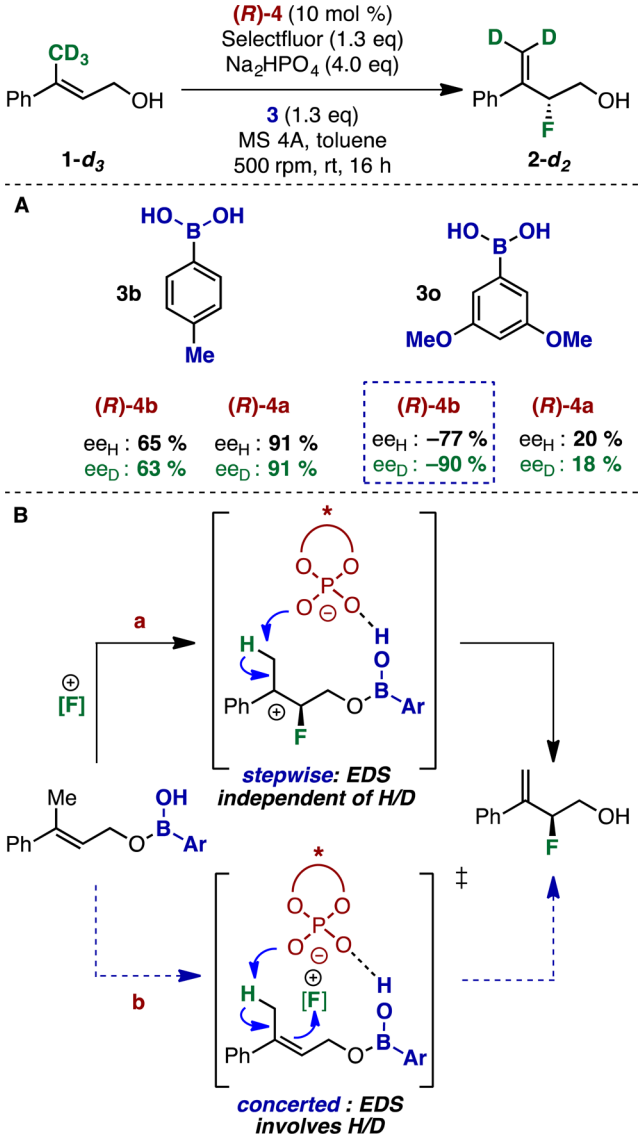


**Figure 7.** (A) Comparison of enantioselectivities of **2** and **2**-$d_2$ for various BA and PA combinations. All reactions were conducted on 0.05 mmol scale with respect to allylic alcohol **1**. (B) Plausible mechanistic rationale for variable dependence of enantioselectivity on isotopic substitution.

demonstrates that phosphate structure also plays a role in this interaction. We thus focused our efforts on identifying the nature of the specific interaction(s) that were presumably responsible for the large inversion of enantioselectivity observed using **3o** with **4b**.

**Probing Direct Interaction.** Inspection of our original data set (Figure 4) revealed that 3,5-disubstituted BAs generally resulted in inverted enantioselectivities when used in combination with **4b**, but this effect appeared particularly pronounced with 3,5-$(OMe)_2$-substituted boronic acid derivative **3o**. In order to distinguish whether this marked effect using **3o** was simply a result of its steric profile or was due to a direct interaction with the methoxy substituent, hybrid 3-Me-5-OMe-substituted phenyl BA derivative **3w** was prepared and evaluated under the standard reaction conditions using each of the catalysts from the original data set. The resulting enantioselectivities are presented in Figure 8A, alongside those obtained using 3,5-$(OMe)_2$ and 3,5-$(Me)_2$ substituted deriva-


DOI: 10.1021/jacs.6b00356
J. Am. Chem. Soc. 2016, 138, 3863−3875

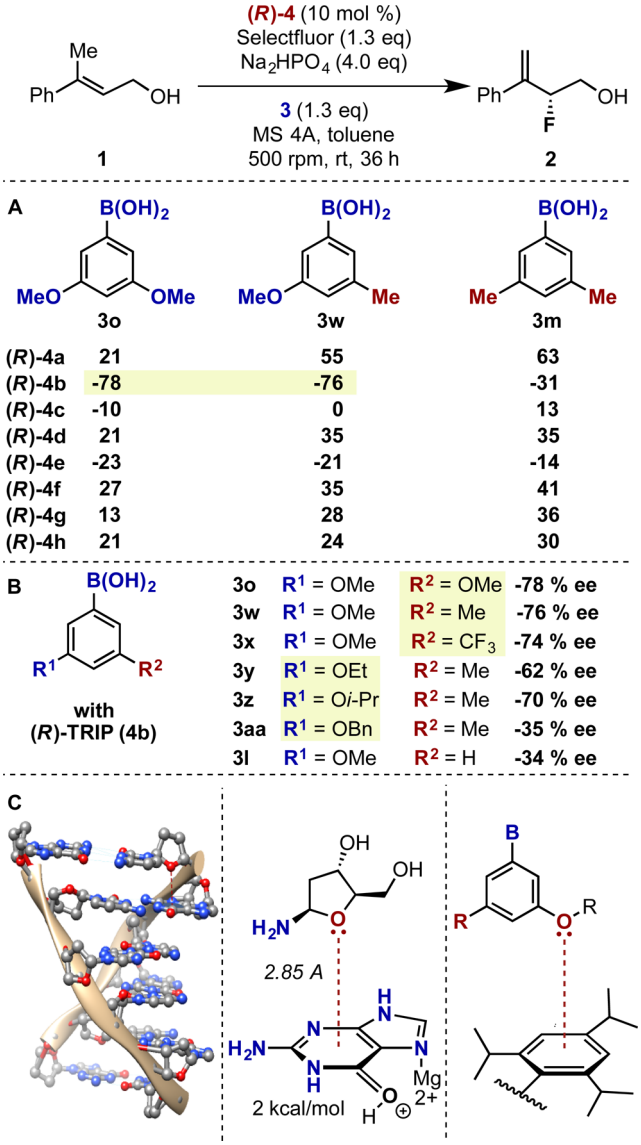


**Figure 8.** (A) Comparison of enantioselectivity of **2** obtained using hyrid BA 3w versus versus **3o** and **3m** as a function of catalyst structure. (B) Effect of variation of alkyl vs alkoxy substituents for various 3,5-disubstituted hybrid phenylboronic acid derivatives. All reactions were conducted on 0.05 mmol scale with respect to allylic alcohol **1**. (C) Left: Qualitative depiction of lone pair-$\pi$ interaction as a stabilizing element for the structure of Z-DNA.[108,109] Right: Qualitative description of potential lone pair-$\pi$ interaction between BA and PA.

tives **3o** and **3m** respectively for comparison. With all catalysts other than **4b**, hybrid BA **3w** afforded the fluorinated product with enantioselectivity similar to that observed with 3,5-$(Me)_2$ substituted variant **3m**, suggesting that the BA steric profile is the dominant factor governing enantioselectivity in these cases. However, in combination with **4b**, **3w** behaved nearly identically to 3,5-$(OMe)_2$ substituted variant **3o**, suggesting the presence of a specific interaction between the BA methoxy group and the aryl substituent of **4b**, which is further supported by the results provided in Figure 8B. Employing a series of hybrid 3,5-disubstituted BAs, holding the alkoxy substituent constant ($R^1$ = OMe) while varying the second substituent ($R^2$ = OMe, Me, $CF_3$) displayed a minimal effect on enantioselectivity. However, for the inverse set of experiments in which the alkyl substituent was held constant ($R^2$ = Me), variation of the alkoxy group ($R^1$ = OEt, O*i*-Pr, OBn) had a significant impact on enantioselectivity, consistent with a structural perturbation at this position disrupting the interaction responsible for the observed inverted enantioselectivity. Notably, 3-OMe substituted BA **3l** also afforded inverted enantioselectivity but to a lesser degree (−34% ee), suggesting that while an interaction with the methoxy group is present, the overall steric profile of the 3,5-substituted derivatives does play a role. Finally, an intriguing dependence of the interaction in question on catalyst structure was observed. Particularly notable was the observation that mesityl-substituted catalyst **4a**, which possesses the same substitution pattern as **4b**, did not furnish **2** with inverted selectivity when used in combination with BA **3o** (Figure 8A). However, an intermediate enantioselectivity value was obtained using hybrid BA **3w** compared with **3o** and **3m** (55% ee vs 21 and 63% ee respectively), suggesting that the putative direct interaction may be present, but attenuated.

On the basis of the following observations, we propose that a lone pair-$\pi$ interaction[108−126] (Figure 8C) is attenuating enantioselectivity: (1) our experiments isolated the interaction to an alkoxy group at a specific position of the aryl BA, (2) variation of this alkoxy group resulted in drastically altered selectivity, and (3) subtle changes to the catalyst aryl ring had a considerable impact on enantioselectivity. First discovered as a stabilizing element for the conformation of Z-DNA (Figure 8C),[118] the lone pair-$\pi$ interaction entails an overlap between a heteroatom lone pair and the face of an aromatic ring, and has been demonstrated to be highly dependent on the geometries of both interacting partners.[127] Several studies have reported the ability of this interaction to alter the overall geometries of molecular complexes by acting in cooperation with other noncovalent interactions such as hydrogen bonding.[115−117,119,122] Although lone pair-$\pi$ interactions have been implicated as stereocontrolling elements in asymmetric catalysis computationally,[125,126] our results serve as compelling experimental support to this end.

We hypothesized that, if an interaction between a methoxy lone pair in **3o** and the catalyst aryl ring were important, then control of the orientation of this ring might provide a means to enhance it. Given the apparent trend moving from **4a** to **4b**, we reasoned that a catalyst with bulkier substituents at the 2,4,6-positions of its aryl rings may serve to reinforce the interaction in question due to better overlap, perhaps owing to a change in the torsional angle between the substituent and the binaphthyl backbone. To this end, 2,4,6-$(Cy)_3$-Ph substituted catalyst (***R***)-**TCYP** (**4i**) was employed with **3o**, furnishing (***S***)-**2** in −92% ee (Scheme 1). Using this same catalyst with the BA that gave the largest positive enantioselectivity in the initial screen with **TRIP** (**4b**) (4-*i*-Bu-substituted variant **3e**), resulted in the formation of (***R***)-**2** in 77% ee. Thus, simply by making a subtle structural change to an achiral additive, we are able to tune the enantiomeric excess of fluorinated product **2** from 77% to −92% (a $\Delta\Delta G^{\ddagger}$ range of 3 kcal/mol) using the same chiral catalyst **4i**. We attribute this remarkable inversion of enantioselectivity to a subtle, noncovalent interaction between the achiral additive and the chiral catalyst.

**Trend Analysis.** Having gained sufficient insight regarding several mechanistic regimes in the data set, we sought to address our initial goal of producing multivariate correlations to describe the catalyst-substrate enantioselectivity imparting interactions (*vide supra*). Examination of Figure 4 revealed that the catalysts that were the most sensitive to changes in the


DOI: 10.1021/jacs.6b00356
J. Am. Chem. Soc. 2016, 138, 3863−3875

**Scheme 1. Inversion of Enantioselectivity of 2 Using Catalyst 4i Changing Only BA Structure**[a]

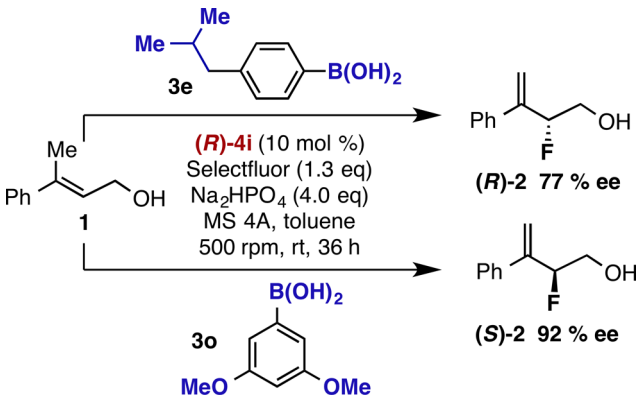


[a]Reactions were conducted on 0.05 mmol scale with respect to allylic alcohol **1**.

BA structure were **4a** (2,4,6-$(Me)_3$-Ph, 3 to 90% ee), **4b** (2,4,6-$(i\text{-}Pr)_3$-Ph, −78 to 66% ee), and **4e** (4-(*i*-Pr)-Ph, −60 to 8% ee). As previously discussed, catalyst **4e** likely operates in a mechanistically distinctive fashion and cannot be compared directly with the others. The remainder of the catalysts tested (**4c**, **4d**, **4f**–**h**) generally displayed ee values over a smaller range indicating less sensitivity to the structure of the BA and were therefore not considered for modeling purposes. Thus, **4a** and **4b** were selected for modeling, along with their 2,4,6-$(Cy)_3$-Ph substituted analogue **4i**. Figure 9A displays the enantioselectivity trend for each catalyst as a function of BA structure. The behavior of all three catalysts is clearly similar for 2- and 4- substituted BAs (Figure 9A, left), indicating the same interactions are likely involved in determining selectivity in this mechanistic region. However, upon moving to the 3,5-substituted BAs (Figure 9A, right) there is a noticeable break in the behavior of **4a** relative to **4b** and **4i** demonstrating that the latter two are behaving differently than **4a**. Thus, to aid the construction of correlations describing these trends, the data set was initially divided according to the BA substitution pattern, separating the 2- and 4- from 3,5-substituted aryl BAs (Figure 9B).

The first set, consisting of 2- and 4-substituted aryl BAs (Figure 9B, light blue, Figure 9C), can be modeled using three descriptors that are sensitive to the structures of the reactive partners: the minimal and maximal width Sterimol[128] steric parameters ($\mathbf{B_1}$ and $\mathbf{B_5}$) describe the BA structure, and the torsion angle between the binaphthyl backbone and 3,3′-substituent describe the catalyst structure. As these are normalized models (see Supporting Information for details), the correlation coefficients denote the relative magnitude of each effect. Thus, we propose that in this region of the data set, the location of the BA substituent and the accessible conformations of the catalyst aryl rings (represented by the catalyst torsion parameter) dictate the geometry of their interaction at the selectivity determining TS.

Although a statistically robust model was identified for the full set of 3,5-substituted BAs (Figure 9D, gray), in addition to catalyst torsion, several BA steric parameters are required to capture the possible TS geometries. Overall, this model seems complex and reveals little regarding the interactions at the origin of asymmetric induction. Thus, this set was further subdivided according to substitution pattern: those with symmetric substitution or any methoxy substituent (Figure 9E, blue) and those with 3-alkoxy-5-methyl substitution (Figure 9F, purple). In line with probing a putative lone pair-$\pi$ interaction, this subdivision keeps the alkoxy substituent constant in one set and the alkyl substituent constant in the other. Although these two models both contain the same molecular descriptors (BA length, **L**, and catalyst torsion angle), the correlation coefficients of each are slightly different, and the former contains an interaction cross-term (consisting of the infrared BA ring stretch ($\nu_3$)[129] and catalyst torsion, Figure 9E). This cross-term may be necessary to differentiate members of this set containing a methoxy substituent from the other BAs, as the former are presumed to undergo a direct interaction with the catalyst. However, in the 3-alkoxy-5-methyl set (Figure 9F), all of the BAs are presumed to undergo the same type of interaction with the catalyst, and thus do not require this additional interaction term. It is particularly intriguing that catalyst torsion has the largest coefficient in both of these models (Figure 9E and 9F), as these BAs are proposed to undergo a direct interaction with the catalyst that is highly geometry dependent. Because torsion is a major feature differentiating catalyst **4a** (2,4,6-$(Me)_3$-Ph) from **4b** and **4i** (2,4,6-$(i\text{-}Pr)_3$-Ph and 2,4,6-$(Cy)_3$-Ph respectively), this is also consistent with the divergence in selectivity visibly noticeable in Figure 9A. These results support the hypothesis that a direct, noncovalent interaction controls enantioselectivity in a manner that is greatly affected by the structures of both the BA and PA, and is proposed to be directing the sizable inversion in enantioselectivity.

## ■ CONCLUSION

Often in the field of asymmetric catalysis, there exists an infrequently acknowledged assumption that the trend observed for a particular catalyst with several substrates will hold when structurally analogous catalysts are tested. In fact, it is this line of reasoning that generally drives standard optimization studies. However, in many cases, this assumption does not prove valid. In these instances, the rational design of a data set that takes the structural variation of multiple reaction components into account can greatly facilitate the identification of regions of structural space where trends break down. We contend that such regions signal potential changes in mechanism in a manner analogous to a break in slope in a classical linear free energy relationship. It is through an understanding of the mechanistic underpinnings of these phenomena that the remainder of the data set can be contextualized. Furthermore, we contend that this approach facilitates the identification of specific data set outliers that would be difficult to design *de novo*, but which can be optimized once identified. Here, we have demonstrated these principles using a data set of enantioselectivities from an asymmetric BA-directed phosphate-catalyzed fluorination of allylic alcohols. We initially set out to understand the structural underpinnings of enantioselectivity by producing statistical models to describe the entire data set. However, the recognition that multiple mechanistic pathways may be operative called for a re-evaluation of our strategy. Guided by a highly organized data set that was designed according to geometric, steric, and electronic criteria, we promptly recognized that not all of the values were directly comparable, presumably due to differences in the mechanisms of asymmetric induction. A series of mechanistic experiments was conducted that shed light on the structural origins of these effects, ultimately leading to a catalytic system capable of


DOI: 10.1021/jacs.6b00356
J. Am. Chem. Soc. 2016, 138, 3863−3875

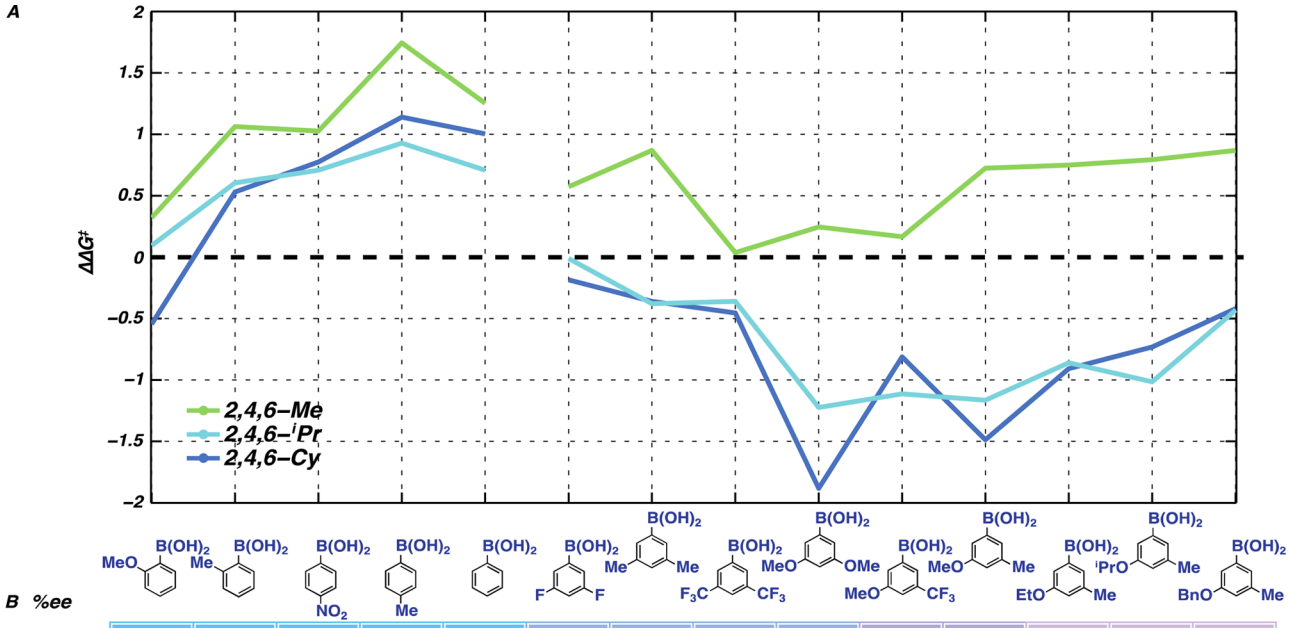


B %ee

| | | | | | | | | | | | | | |
|---|---|---|---|---|---|---|---|---|---|---|---|---|---|
| 2,4,6-Me | 26.5 | 71.5 | 70 | 90 | 78.5 | 45 | 62.5 | 3 | 20.5 | 14 | 54.5 | 56 | 58.5 | 62.5 |
| 2,4,6-iPr | 8 | 47 | 53.5 | 65.5 | 53.5 | -1 | -31 | -29.5 | -77.5 | -73.5 | -75.5 | -62 | -69.5 | -35 |
| 2,4,6-Cy | -43 | 42 | 57.5 | 74.5 | 69 | -15.5 | -29.5 | -36.5 | -92 | -59.5 | -85 | -64.5 | -55 | -34 |

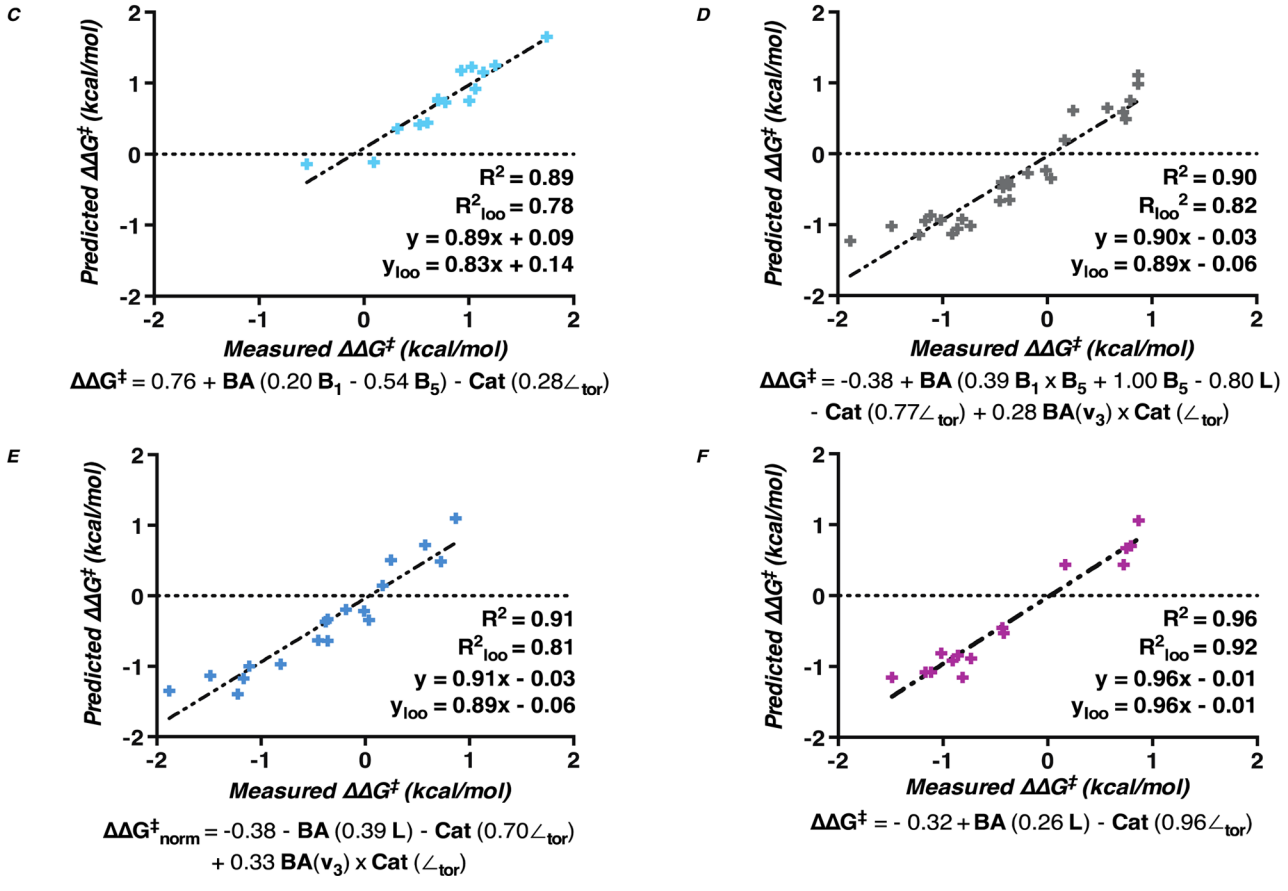


**Figure 9.** (A) Graphical representation of catalyst structure-selectivity trends as a function of BA structure. (B) Enantioselectivity of **2** using catalysts bearing 2,4,6-trisubstituted aryl substituents with various BAs. (C–F) Mathematical correlation of normalized catalyst and BA molecular descriptors to enantioselectivity ($\Delta\Delta G^{\ddagger}$) for 2- and 4-substituted aryl BAs (C), all 3,5-disubstituted aryl BAs (D), 3,5-disubstituted aryl BAs with symmetrical substitution or a methoxy substituent (E), and 3-alkoxy-5-methyl substituted aryl BAs (F). All reactions were conducted on 0.05 mmol scales with respect to allylic alcohol **1**.



DOI: 10.1021/jacs.6b00356
J. Am. Chem. Soc. 2016, 138, 3863–3875

producing either enantiomer of a chiral fluorinated building block in high enantioselectivity. The insights gained in this study can be generalized to countless situations in which structural features of the catalysts and substrates may alter the mechanism through which selectivity is induced. It is our current goal to apply these approaches to new reaction development, facilitating both a foundational guide to catalyst design and a rapid identification of mechanistic outliers.

## ■ ASSOCIATED CONTENT

### Supporting Information

The Supporting Information is available free of charge on the ACS Publications website at DOI: 10.1021/jacs.6b00356.

Table of parameters. (XLSX)
Example model development script. (TXT)
Experimental and modeling details and characterization data. (PDF)

## ■ AUTHOR INFORMATION


### Corresponding Authors

*sigman@chem.utah.edu
*fdtoste@berkeley.edu

### Author Contributions

‖AJN and AM contributed equally.


### Notes

The authors declare no competing financial interest.

## ■ ACKNOWLEDGMENTS

We thank the NSF (CHE-0749506 and CHE-1361296) and the National Institute of General Medical Sciences (R01 GM104534) for partial support of this work. The support and resources from the Center for High Performance Computing at the University of Utah are gratefully acknowledged. Eiji Yamamoto, Matt Larsen, Weiwei Zi, and Willie Wolf are acknowledged for helpful discussions.

## ■ REFERENCES


(1) Seeman, J. I. *Chem. Rev.* **1983**, *83* (2), 83.
(2) Milo, A.; Neel, A. J.; Toste, F. D.; Sigman, M. S. *Science* **2015**, *347* (6223), 737.
(3) Knowles, R. R.; Jacobsen, E. N. *Proc. Natl. Acad. Sci. U. S. A.* **2010**, *107* (48), 20678.
(4) Jaffé, H. H. *Chem. Rev.* **1953**, *53* (2), 191.
(5) Schreck, J. O. *J. Chem. Educ.* **1971**, *48* (2), 103.
(6) Hoz, S.; Ben-Zion, M. *J. Chem. Soc., Chem. Commun.* **1980**, *10*, 453.
(7) Sjöström, M.; Wold, S.; Fredga, A.; Bonner, W. A.; Örn, U. *Acta Chem. Scand.* **1981**, *35b*, 537.
(8) Jencks, W. P.; Brant, S. R.; Gandler, J. R.; Fendrich, G.; Nakamura, C. *J. Am. Chem. Soc.* **1982**, *104* (25), 7045.
(9) Williams, A. In *New Comprehensive Biochemistry*; Page, M. I., Ed.; The Chemistry of Enzyme Action; Elsevier, 1984; Vol. *6*, pp 127−201.
(10) Greig, I. R. *Chem. Soc. Rev.* **2010**, *39* (6), 2272.
(11) Swain, C. G.; Langsdorf, W. P. *J. Am. Chem. Soc.* **1951**, *73* (6), 2813.
(12) Anderson, B. M.; Jencks, W. P. *J. Am. Chem. Soc.* **1960**, *82* (7), 1773.
(13) Hart, H.; Sedor, E. A. *J. Am. Chem. Soc.* **1967**, *89* (10), 2342.
(14) Ta-Shma, R.; Rappoport, Z. *J. Am. Chem. Soc.* **1977**, *99* (6), 1845.
(15) Young, P. R.; Jencks, W. P. *J. Am. Chem. Soc.* **1979**, *101* (12), 3288.
(16) Stein, A. R.; Tencer, M.; Moffatt, E. A.; Dawe, R.; Sweet, J. *J. Org. Chem.* **1980**, *45* (17), 3539.
(17) Bergon, M.; Calmon, J.-P. *Tetrahedron Lett.* **1981**, *22* (10), 937.
(18) Richard, J. P.; Jencks, W. P. *J. Am. Chem. Soc.* **1982**, *104* (17), 4689.
(19) Meenakshisundaram, S.; Sockalingam, R. *Collect. Czech. Chem. Commun.* **2001**, *66* (6), 897.
(20) Um, I.-H.; Han, H.-J.; Ahn, J.-A.; Kang, S.; Buncel, E. *J. Org. Chem.* **2002**, *67* (24), 8475.
(21) Ravi, R.; Sanjeev, R.; Jagannadham, V. *Int. J. Chem. Kinet.* **2013**, *45* (12), 803.
(22) Jmaoui, I.; Boubaker, T.; Goumont, R. *Int. J. Chem. Kinet.* **2013**, *45* (3), 152.
(23) Ciaccia, M.; Pilati, S.; Cacciapaglia, R.; Mandolini, L.; Di Stefano, S. *Org. Biomol. Chem.* **2014**, *12* (20), 3282.
(24) Lutz, F.; Igarashi, T.; Kawasaki, T.; Soai, K. *J. Am. Chem. Soc.* **2005**, *127* (35), 12206.
(25) Lutz, F.; Igarashi, T.; Kinoshita, T.; Asahina, M.; Tsukiyama, K.; Kawasaki, T.; Soai, K. *J. Am. Chem. Soc.* **2008**, *130* (10), 2956.
(26) Holland, M. C.; Metternich, J. B.; Daniliuc, C.; Schweizer, W. B.; Gilmour, R. *Chem. - Eur. J.* **2015**, *21* (28), 10031.
(27) Phipps, R. J.; Hamilton, G. L.; Toste, F. D. *Nat. Chem.* **2012**, *4* (8), 603.
(28) Mahlau, M.; List, B. *Angew. Chem., Int. Ed.* **2013**, *52* (2), 518.
(29) Brak, K.; Jacobsen, E. N. *Angew. Chem., Int. Ed.* **2013**, *52* (2), 534.
(30) Rauniyar, V.; Lackner, A. D.; Hamilton, G. L.; Toste, F. D. *Science* **2011**, *334* (6063), 1681.
(31) Phipps, R. J.; Hiramatsu, K.; Toste, F. D. *J. Am. Chem. Soc.* **2012**, *134* (20), 8376.
(32) Wang, Y.-M.; Wu, J.; Hoong, C.; Rauniyar, V.; Toste, F. D. *J. Am. Chem. Soc.* **2012**, *134* (31), 12928.
(33) Honjo, T.; Phipps, R. J.; Rauniyar, V.; Toste, F. D. *Angew. Chem., Int. Ed.* **2012**, *51* (38), 9684.
(34) Phipps, R. J.; Toste, F. D. *J. Am. Chem. Soc.* **2013**, *135* (4), 1268.
(35) Shunatona, H. P.; Früh, N.; Wang, Y.-M.; Rauniyar, V.; Toste, F. D. *Angew. Chem., Int. Ed.* **2013**, *52* (30), 7724.
(36) Neel, A. J.; Hehn, J. P.; Tripet, P. F.; Toste, F. D. *J. Am. Chem. Soc.* **2013**, *135* (38), 14044.
(37) Wu, J.; Wang, Y.-M.; Drljevic, A.; Rauniyar, V.; Phipps, R. J.; Toste, F. D. *Proc. Natl. Acad. Sci. U. S. A.* **2013**, *110* (34), 13729.
(38) Lackner, A. D.; Samant, A. V.; Toste, F. D. *J. Am. Chem. Soc.* **2013**, *135* (38), 14090.
(39) Liu, H.; Jiang, G.; Pan, X.; Wan, X.; Lai, Y.; Ma, D.; Xie, W. *Org. Lett.* **2014**, *16* (7), 1908.
(40) Romanov-Michailidis, F.; Guénée, L.; Alexakis, A. *Angew. Chem., Int. Ed.* **2013**, *52* (35), 9266.
(41) Romanov-Michailidis, F.; Guénée, L.; Alexakis, A. *Org. Lett.* **2013**, *15* (22), 5890.
(42) Yang, X.; Phipps, R. J.; Toste, F. D. *J. Am. Chem. Soc.* **2014**, *136* (14), 5225.
(43) Nelson, H. M.; Reisberg, S. H.; Shunatona, H. P.; Patel, J. S.; Toste, F. D. *Angew. Chem., Int. Ed.* **2014**, *53* (22), 5600.
(44) Nelson, H. M.; Patel, J. S.; Shunatona, H. P.; Toste, F. D. *Chem. Sci.* **2014**, *6* (1), 170.
(45) Romanov-Michailidis, F.; Pupier, M.; Guénée, L.; Alexakis, A. *Chem. Commun.* **2014**, *50* (88), 13461.
(46) Romanov-Michailidis, F.; Pupier, M.; Besnard, C.; Bürgi, T.; Alexakis, A. *Org. Lett.* **2014**, *16* (19), 4988.
(47) Nelson, H. M.; Williams, B. D.; Miró, J.; Toste, F. D. *J. Am. Chem. Soc.* **2015**, *137* (9), 3213.
(48) Romanov-Michailidis, F.; Romanova-Michaelides, M.; Pupier, M.; Alexakis, A. *Chem. - Eur. J.* **2015**, *21* (14), 5561.
(49) Egami, H.; Asada, J.; Sato, K.; Hashizume, D.; Kawato, Y.; Hamashima, Y. *J. Am. Chem. Soc.* **2015**, *137* (32), 10132.
(50) Akiyama, T. *Chem. Rev.* **2007**, *107* (12), 5744.
(51) Terada, M. *Synthesis* **2010**, *2010* (12), 1929.
(52) Terada, M. *Curr. Org. Chem.* **2011**, *15* (13), 2227.
(53) Mori, K.; Akiyama, T. In *Comprehensive Enantioselective Organocatalysis*; Dalko, P. I., Ed.; Wiley-VCH Verlag GmbH & Co. KGaA, 2013; pp 289−314.




DOI: 10.1021/jacs.6b00356
J. Am. Chem. Soc. 2016, 138, 3863−3875

(54) Parmar, D.; Sugiono, E.; Raja, S.; Rueping, M. *Chem. Rev.* **2014**, *114* (18), 9047.
(55) Zi, W.; Wang, Y.-M.; Toste, F. D. *J. Am. Chem. Soc.* **2014**, *136* (37), 12864.
(56) Bobbio, C.; Gouverneur, V. *Org. Biomol. Chem.* **2006**, *4* (11), 2065.
(57) Shibata, N.; Ishimaru, T.; Nakamura, S.; Toru, T. *J. Fluorine Chem.* **2007**, *128* (5), 469.
(58) Ma, J.-A.; Cahard, D. *Chem. Rev.* **2008**, *108* (9), PR1.
(59) Cahard, D.; Xu, X.; Couve-Bonnaire, S.; Pannecoucke, X. *Chem. Soc. Rev.* **2010**, *39* (2), 558.
(60) Lectard, S.; Hamashima, Y.; Sodeoka, M. *Adv. Synth. Catal.* **2010**, *352* (16), 2708.
(61) Valero, G.; Companyó, X.; Rios, R. *Chem. - Eur. J.* **2011**, *17* (7), 2018.
(62) Ye, Z.; Zhao, G. *Chimia* **2011**, *65* (12), 902.
(63) Yang, X.; Wu, T.; Phipps, R. J.; Toste, F. D. *Chem. Rev.* **2015**, *115* (2), 826.
(64) Li, D. R.; Murugan, A.; Falck, J. R. *J. Am. Chem. Soc.* **2008**, *130* (1), 46.
(65) (a) Although reaction rates were qualitatively greater in the absence of activated molecular sieves, sieves were included in the standard reaction conditions as their presence generally resulted in more reproducible enantioselectivities. Additionally, toluene was used as the only solvent for operational simplicity. See Supporting Information for details. (b) For the entirety of this article, we have defined the result in Figure 1B as the standard enantioselectivity (i.e., the (*S*)-catalyst affords the (*S*)-product). On the basis of this convention, the predominant formation of the (*R*)-product was considered "negative" when using the (*S*)-catalyst. Similarly, if use of the (*R*)-catalyst results in the (*S*) enantiomer as the major product, this result is considered "negative". This convention was opted as it better alerts the reader to the fact that the enantioselectivity inversion is independent of the catalyst enantiomer used (as opposed to the (*R*) and (*S*) terminology).
(66) Hoffmann, S.; Seayad, A. M.; List, B. *Angew. Chem., Int. Ed.* **2005**, *44* (45), 7424.
(67) Tiago Menezes Correia, J. *Synlett* **2015**, *26* (03), 416.
(68) Miller, J. J.; Sigman, M. S. *Angew. Chem., Int. Ed.* **2008**, *47* (4), 771.
(69) Gustafson, J. L.; Sigman, M. S.; Miller, S. J. *Org. Lett.* **2010**, *12* (12), 2794.
(70) Jensen, K. H.; Sigman, M. S. *J. Org. Chem.* **2010**, *75* (21), 7194.
(71) Harper, K. C.; Sigman, M. S. *Proc. Natl. Acad. Sci. U. S. A.* **2011**, *108*, 2179.
(72) Harper, K. C.; Sigman, M. S. *Science* **2011**, *333* (6051), 1875.
(73) Harper, K. C.; Bess, E. N.; Sigman, M. S. *Nat. Chem.* **2012**, *4* (5), 366.
(74) Harper, K. C.; Sigman, M. S. *J. Org. Chem.* **2013**, *78* (7), 2813.
(75) Harper, K. C.; Vilardi, S. C.; Sigman, M. S. *J. Am. Chem. Soc.* **2013**, *135* (7), 2482.
(76) McCammant, M. S.; Sigman, M. S. *Chem. Sci.* **2015**, *6* (2), 1355.
(77) Zhang, C.; Santiago, C. B.; Kou, L.; Sigman, M. S. *J. Am. Chem. Soc.* **2015**, *137* (23), 7290.
(78) Puchot, C.; Samuel, O.; Dunach, E.; Zhao, S.; Agami, C.; Kagan, H. B. *J. Am. Chem. Soc.* **1986**, *108* (9), 2353.
(79) Guillaneux, D.; Zhao, S.-H.; Samuel, O.; Rainford, D.; Kagan, H. B. *J. Am. Chem. Soc.* **1994**, *116* (21), 9430.
(80) Kagan, H. B.; Girard, C.; Guillaneux, D.; Rainford, D.; Samuel, O.; Zhang, S. Y.; Zhao, S. H.; Ciglic, M. I.; Haugg, M.; Trabesinger-Rüf, N.; Weinhold, E. G. *Acta Chem. Scand.* **1996**, *50*, 345.
(81) Heller, D.; Drexler, H.-J.; Fischer, C.; Buschmann, H.; Baumann, W.; Heller, B. *Angew. Chem., Int. Ed.* **2000**, *39* (3), 495.
(82) Kagan, H. B. *Adv. Synth. Catal.* **2001**, *343* (3), 227.
(83) Kagan, H. B. *Synlett* **2001**, *2001* (Special Issue), 888.
(84) Klussmann, M.; Mathew, S. P.; Iwamura, H.; Wells, D. H.; Armstrong, A.; Blackmond, D. G. *Angew. Chem.* **2006**, *118* (47), 8157.
(85) Satyanarayana, T.; Abraham, S.; Kagan, H. B. *Angew. Chem., Int. Ed.* **2009**, *48* (3), 456.
(86) Kitamura, M.; Suga, S.; Oka, H.; Noyori, R. *J. Am. Chem. Soc.* **1998**, *120* (38), 9800.
(87) Chen, Y. K.; Costa, A. M.; Walsh, P. J. *J. Am. Chem. Soc.* **2001**, *123* (22), 5378.
(88) Noyori, R.; Suga, S.; Oka, H.; Kitamura, M. *Chem. Rec.* **2001**, *1* (2), 85.
(89) Buono, F.; Walsh, P. J.; Blackmond, D. G. *J. Am. Chem. Soc.* **2002**, *124* (46), 13652.
(90) Oestreich, M.; Rendler, S. *Angew. Chem., Int. Ed.* **2005**, *44* (11), 1661.
(91) Palomo, C.; Oiarbide, M.; Laso, A. *Angew. Chem., Int. Ed.* **2005**, *44* (25), 3881.
(92) Portada, T.; Roje, M.; Hameršak, Z.; Žinić, M. *Tetrahedron Lett.* **2005**, *46* (35), 5957.
(93) Dziedzic, P.; Zou, W.; Ibrahem, I.; Sundén, H.; Córdova, A. *Tetrahedron Lett.* **2006**, *47* (37), 6657.
(94) Duan, W.-L.; Iwamura, H.; Shintani, R.; Hayashi, T. *J. Am. Chem. Soc.* **2007**, *129* (7), 2130.
(95) Lou, S.; Moquist, P. N.; Schaus, S. E. *J. Am. Chem. Soc.* **2007**, *129* (49), 15398.
(96) Gelalcha, F. G.; Anilkumar, G.; Tse, M. K.; Brückner, A.; Beller, M. *Chem. - Eur. J.* **2008**, *14* (25), 7687.
(97) El-Hamdouni, N.; Companyó, X.; Rios, R.; Moyano, A. *Chem. - Eur. J.* **2010**, *16* (4), 1142.
(98) Li, N.; Chen, X.-H.; Zhou, S.-M.; Luo, S.-W.; Song, J.; Ren, L.; Gong, L.-Z. *Angew. Chem., Int. Ed.* **2010**, *49* (36), 6378.
(99) Chen, Z.; Wang, B.; Wang, Z.; Zhu, G.; Sun, J. *Angew. Chem., Int. Ed.* **2013**, *52* (7), 2027.
(100) Wang, H.-Y.; Zhang, K.; Zheng, C.-W.; Chai, Z.; Cao, D.-D.; Zhang, J.-X.; Zhao, G. *Angew. Chem., Int. Ed.* **2015**, *54* (6), 1775.
(101) Tanaka, K.; Iwashita, T.; Yoshida, E.; Ishikawa, T.; Otuka, S.; Urbanczyk-Lipkowska, Z.; Takahashi, H. *Chem. Commun.* **2015**, *51* (37), 7907.
(102) For further support of this claim, see the Supporting Information.
(103) A significant positive nonlinear effect was also observed using **4e** and *o*-tolylboronic acid (**3p**). See the Supporting Information for details.
(104) Despite its formally "positive" enantioselectivity with *p*-tolylboronic acid (**3b**), Ph-substituted catalyst **4f** displayed a nonlinear effect, as anticipated given its lack of steric bulk proximal to the phosphate moiety. For a more complete discussion of this experiment, see the Supporting Information.
(105) It should also be noted that for both of the BA subsets, $\sigma$-para values correlate with selectivity, indicating that asymmetric induction throughout either set is governed by a substantial resonance component ($\sigma$-meta values were not well-correlated, see Supporting Information for details).
(106) Martínez-Aguirre, M. A.; Yatsimirsky, A. K. *J. Org. Chem.* **2015**, *80* (10), 4985.
(107) Tokunaga, Y.; Ueno, H.; Shimomura, Y.; Seo, T. *Heterocycles* **2002**, *57* (5), 787.
(108) Egli, M.; Sarkhel, S. *Acc. Chem. Res.* **2007**, *40* (3), 197.
(109) Singh, S. K.; Das, A. *Phys. Chem. Chem. Phys.* **2015**, *17* (15), 9596.
(110) Gallivan, J. P.; Dougherty, D. A. *Org. Lett.* **1999**, *1* (1), 103.
(111) Grimme, S. *J. Comput. Chem.* **2004**, *25* (12), 1463.
(112) Amicangelo, J. C.; Gung, B. W.; Irwin, D. G.; Romano, N. C. *Phys. Chem. Chem. Phys.* **2008**, *10* (19), 2695.
(113) Jain, A.; Ramanathan, V.; Sankararamakrishnan, R. *Protein Sci.* **2009**, *18* (3), 595.
(114) Yang, T.; An, J.-J.; Wang, X.; Wu, D.-Y.; Chen, W.; Fossey, J. S. *Phys. Chem. Chem. Phys.* **2012**, *14* (30), 10747.
(115) Singh, S. K.; Kumar, S.; Das, A. *Phys. Chem. Chem. Phys.* **2014**, *16* (19), 8819.
(116) Mondal, S. I.; Dey, A.; Sen, S.; Patwari, G. N.; Ghosh, D. *Phys. Chem. Chem. Phys.* **2014**, *17* (1), 434.
(117) Ao, M.-Z.; Tao, Z.; Liu, H.-X.; Wu, D.-Y.; Wang, X. *Comput. Theor. Chem.* **2015**, *1064*, 25.


DOI: 10.1021/jacs.6b00356
*J. Am. Chem. Soc.* 2016, 138, 3863−3875

(118) Egli, M.; Gessner, R. V. *Proc. Natl. Acad. Sci. U. S. A.* **1995**, *92* (1), 180.
(119) Korenaga, T.; Tanaka, H.; Ema, T.; Sakai, T. *J. Fluorine Chem.* **2003**, *122* (2), 201.
(120) Gung, B. W.; Xue, X.; Reich, H. J. *J. Org. Chem.* **2005**, *70* (18), 7232.
(121) Gung, B. W.; Zou, Y.; Xu, Z.; Amicangelo, J. C.; Irwin, D. G.; Ma, S.; Zhou, H.-C. *J. Org. Chem.* **2008**, *73* (2), 689.
(122) Korenaga, T.; Shoji, T.; Onoue, K.; Sakai, T. *Chem. Commun.* **2009**, *31*, 4678.
(123) Nijamudheen, A.; Jose, D.; Shine, A.; Datta, A. *J. Phys. Chem. Lett.* **2012**, *3* (11), 1493.
(124) Pavlakos, I.; Arif, T.; Aliev, A. E.; Motherwell, W. B.; Tizzard, G. J.; Coles, S. J. *Angew. Chem., Int. Ed.* **2015**, *54* (28), 8169.
(125) Duarte, V. C. M.; Faustino, H.; Alves, M. J.; Gil Fortes, A.; Micaelo, N. *Tetrahedron: Asymmetry* **2013**, *24* (18), 1063.
(126) Reddi, Y.; Sunoj, R. B. *ACS Catal.* **2015**, *5* (3), 1596.
(127) Mooibroek, T. J.; Gamez, P.; Reedijk, J. *CrystEngComm* **2008**, *10* (11), 1501.
(128) Verloop, A.; Hoogenstraaten, W.; Tipker, J. In *Drug Design*; Ariëns, E. J., Ed.; Medicinal Chemistry: A Series of Monographs; Academic Press: Amsterdam, 1976; Vol. *11*, Part G, pp 165−207.
(129) Milo, A.; Bess, E. N.; Sigman, M. S. *Nature* **2014**, *507* (7491), 210.



DOI: 10.1021/jacs.6b00356
*J. Am. Chem. Soc.* 2016, 138, 3863−3875